Effect of Molecular Weight and Ionic Strength on the Formation of Polyelectrolyte Complexes Based on Poly(methacrylic acid) and Chitosan

C. L. de Vasconcelos, P. M. Bezerril, D. E. S. dos Santos, T. N. C. Dantas, M. R. Pereira, and J. L. C. Fonseca*

Departamento de Química, Universidade Federal do Rio Grande do Norte, Campus Universitário, Lagoa Nova, RN 59078-970, Brazil

Received December 18, 2005; Revised Manuscript Received February 3, 2006

Chitosan/poly(methacrylic acid) complexes, CS/PMAA, were prepared via dropwise addition of a solution of PMAA to a solution of chitosan in acetic acid 2 wt %. The increase in molecular weight of PMAA inhibited the formation of insoluble complexes, while the increase in ionic strength first favored the formation of the complex followed by inhibiting it at higher concentrations. These observations were related to a description of polyelectrolyte complexation that was strongly dependent on macromolecular dimensions, both in terms of molecular weight and of coil expansion/contraction driven by polyelectrolyte effect.

1. Introduction

Macromolecular complexes with the subsequent formation of particulate systems with micrometric and submicrometric dimensions, generally in the form of colloids or suspensions obtained by polymerization, aggregation, and/or complexation of polymers, have been reported as promising advanced functional materials.[1] These polymer dispersions have been used in a wide variety applications, such as in the preparation of synthetic rubber,[2] coatings,[3] adhesives for paper and textile,[4,5] flocculants,[6,7] and rheological modifiers.[8] They have also been increasingly used in biomedical and pharmaceutical applications, such as diagnostic tests and targeted drug delivery.[9−11]

In the specific field of biomedicine, one requires natural and synthetic polymers that are biocompatible, biodegradable, capable of binding with proteins, genes, nucleic acids, acidic lipids as well as having the ability of absorption enhancing and mucosal adhesion without toxicity.[12] To use them for the incorporation of bioactive macromolecules and vaccines such as monoclonal bodies, plasmids, antigens, oligonucleotides, enzymes, recombinant proteins, and peptides for therapeutic applications, the design/preparation of these systems must be monitored in terms of particle shape and morphology, size distribution, surface chemistry, and polymer nature.[13]

Among all methods of development of polymer dispersions for biomedicine, the employment of polyelectrolyte complexes represents a very attractive approach, mainly due to the simplicity involved in the preparation.[14] Among these complexes, the combination of chitosan (a mucoadhesive cationic polyelectrolyte) and poly(methacrylic acid) with natural and synthetic macromolecules has received considerable attention.[15] Chitosan is a natural linear copolymer of β-(1→4)-2-amino-2-deoxy-D-glucopyranose and β-(1→4)-2-acetamido-2-deoxy-D-glucopyranose, derived from the partial alkaline *N*-deacetylation of chitin [poly(β-(1→4)-2-acetamido-2-deoxy-D-glucopyranose)], an abundant mucopolysaccharide present in the outer shell of crustaceans.[16] Poly(methacrylic acid) is a biocompatible synthetic polyelectrolyte with polyanionic character.[17] When ionized, both polyelectrolytes have intrinsic biological properties. Chitosan is able to increase intestinal permeability of macromolecules and particles through intercellular spaces.[18] On the other hand, an important feature of the resulting polyacrylates is that they are able to inhibit the proteolytic activity of the luminal endopeptidases trypsin and α-chymotrypsin and the exopeptidases carboxypeptidase A and cytosolic aminopeptidase by the depletion of the essential cofactors Ca^{2+} (in endopeptidases) and Zn^{2+} (in exopeptidases) out of the enzyme structure.[19] Depletion of the extracellular Ca^{2+} by polyacrylates also influences the intactness of epithelial tight junction.[20] The decrease in extracellular Ca^{2+} concentration brings in morphological alterations in the expression of the F-actin cytoskeleton, as well as in the localization of tight functional junctional proteins, also resulting in the enhancement of paracellular permeability.[20,21]

A considerable number of factors related to the polymer structural features and environmental parameters has been established on the formation of polyelectrolyte complexes. Regarding the effect of polyelectrolyte molecular dimensions, Becherán-Marón et al. have investigated the stoichiometry and complexation degree of the products of the reaction between chitosan and alginate.[22] They observed that there was no dependence of alginate chemical composition and molecular weight of chitosan on complex formation. Janes and Alonso have developed a chitosan nanoparticulated system based on ionotropic gelation with sodium tripolyphosphate (TPP) and found that the molecular weight of chitosan was a determining factor for some physicochemical properties of the dispersions, such as nanoparticle size and zeta potential, ζ.[23] Using a similar method with TPP, Ko et al. have also reported that the molecular weight of chitosan affected microparticle size and surface morphology:[24] higher chitosan molecular weights were correlated to more spherical microparticles, with the particle size ranging from 500 to 700 μm.

The influence of ionic strength of the disperser phase has been analyzed for different polyelectrolyte systems, to correlate the presence of low molecular weight salts to the formation of

* To whom correspondence should be addressed. Fax: +55 (0)84 3211 9224. Phone: +55 (0)84 3215 3828 ext. 215. E-mail: jlcfonseca@uol.com.br.

10.1021/bm050963w CCC: $33.50
Published on Web 03/22/2006

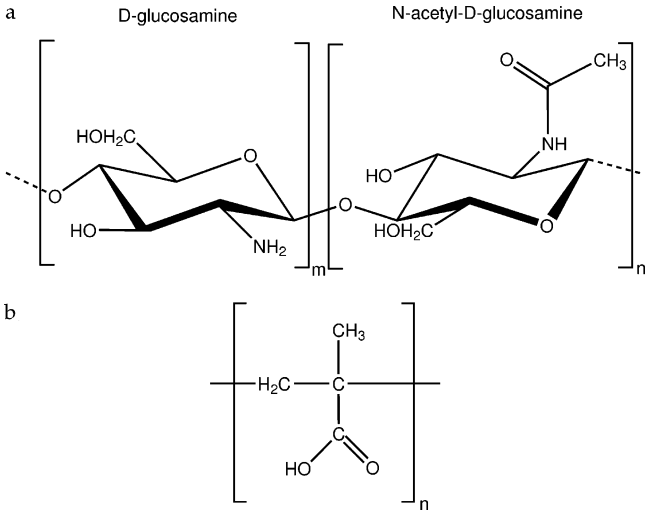

Figure 1. Chemical structure of chitosan (a) and poly(methacrylic acid) (b). In chitosan, the two monomers D-glucosamine and *N*-acetyl-D-glucosamine are randomly distributed and for a degree of deacetylation of 90%, $m/(m + n) = 0.9$.

polyelectrolyte macromolecular complexes.[25,26] The emphasis in this class of studies is the characterization of aggregation processes in suspensions of charged colloidal particles in the presence of oppositely charged polyelectrolytes as well as the dissociation effect on the polyelectrolyte complexes and/or polyelectrolyte surfactant complexes at a critical range of ionic strength and/or ionic valence of the salts.[27−29]

Chitosan−poly(acrylic acid) polyelectrolyte complexes have already been prepared in aqueous systems,[29−31] although there have been no attempts to explore the effects of ionic strength and molecular weight of the polyacrylate derivative polyanion as the shell surface agent in polyelectrolyte systems obtained with chitosan as a polysaccharide core agent. In this work, polyelectrolyte complexes based on polyelectrolytes having weak ionic groups were obtained by mixing them in non-stoichiometric ratios in saltless aqueous solution and in aqueous solutions of low molecular weight salt. The behavior of the resultant complexes and the range of mixing ratio was studied employing viscosity and turbidity measurements, surface charge analysis, FTIR spectroscopy being used for chemically characterize the obtained complexes.

2. Experimental Section

2.1. Materials. Chitosan, CS, (Polymar Ltda, Brazil) used in this work had a deacetylation degree of ca. 90% and a molecular weight $\bar{M}_v \approx 2.9 \times 10^5$ g·mol^{-1} (determined using Mark-Howink-Sakurada equation from viscometric data[32]). Methacrylic acid (Aldrich, Germany) and potassium peroxydisulfate (P. A., Vetec, Brazil) were used as received. The chemical structures of chitosan and methacrylic acid are shown in Figure 1.

2.2. Polymerization in aqueous Solution. It is known that, in free radical polymerizations, molecular weight is regulated by temperature, initiator concentration, and the way both initiator and monomer are fed to the system.[33] To synthesize poly(methacrylic acid), PMAA, with different average molecular weights, use was made of the last two variables. Methacrylic acid, MAA, was solubilized in bidistilled water so that an aqueous solution of MAA 5 wt % was obtained. Potassium peroxydisulfate, $K_2S_2O_8$, was added to the solution and the polymerization was carried out at 90 °C, for 3 h. Two different polymerizations were carried out.

1. The amount of initiator used (in terms of mass percentage of MAA) was 1.5 wt %: one-third added at the beginning of the polymerization, one-third after the first hour of polymerization, and the remaining initiator after the second hour of polymerization;

2. An initiator/MAA mass ratio of 0.375% was used: one-third added at the beginning of the polymerization, one-third after the first hour of polymerization, and the remaining initiator after the second hour of polymerization.

During the polymerization, the polyacid solution became turbid, turning into a translucid solution clear again when cooled under stirring to room temperature. Solid PMAA was obtained from precipitation of the polyacid from its clear solution with diethyl ether, at room temperature. Although diethyl ether is a solvent of low polarity with a solubility ca. 1.5% in water, it can undergo hydrogen bonding with PMAA: when we added it to the PMAA solution, a tacky precipitate was formed and repeatedly washed with diethyl-ether. This rubberous mass was then dried in an oven at the temperature of ≈ 60 °C. Aqueous stock solutions of 7 wt % were obtained (the exact concentration was determined by titration with NaOH).

Intrinsic viscosity, $[\eta]$, from aqueous solution of PMAA was obtained using an Ubbelohde viscometer size 0B. Polyelectrolyte effect[34] was suppressed by making the measurements in dioxane.[35,36] The efflux time in these measurements was never shorter than 100 seconds [the efflux time of dioxane being 267.8 ± 0.1 s]. All these experiments were conducted at a temperature $T = 25.00 \pm 0.05$ °C. The simultaneous linearizations of equations[37]

$$\eta_{red} = [\eta] + k'[\eta]^2 c \quad (1)$$

and

$$\eta_{inh} = [\eta] + \left(k' - \frac{1}{2}\right)[\eta]^2 c \quad (2)$$

where η_{red} and η_{inh} are respectively the reduced and inherent viscosity numbers, allowed one to determine the values of intrinsic viscosity, $[\eta]$, and k_1 for PMAA of different molecular weights.

2.3. Preparation of CS/PMAA Particles. CS/PMAA particles were obtained from positively charged CS and negatively charged PMAA by the dropping method. A solution of 0.02% CS (pH = 2.60 ± 0.05; CS was dissolved in 2 wt % acetic acid solution and filtered through a Millipore Millex 41 μm filter, prior to use) was added dropwise to a 0.02% PMAA aqueous solution (pH = 3.70 ± 0.05). An opalescent suspension was instantaneously formed under magnetic stirring, depending on the amount of CS solution added. The resultant dispersion was additionally stirred for 1 h at room temperature, before taking for further experiments. The variables in the experiments were the mass ratio of CS to PMAA, $r_{CS/PMAA}$ (or the molar ratio of NH_2 from chitosan to COOH from PMAA, $r_{NH_2/COOH}$), the molecular weight of PMAA (indirectly monitored via the PMAA intrinsic viscosity, $[\eta]$), and ionic strength, which is expressed as[38]

$$I_C = \frac{1}{2}\sum_i C_i z_i^2 \quad (3)$$

where C_i is the concentration of ion i and z_i is its valence. For computation of ionic strength, one should take into account the H_3O^+ and COO^- ions from the acetic acid solution. Since the concentrations of these ions were constant, ionic strength was indirectly monitored via the concentration of added NaCl, C_{NaCl}, which were 1.00×10^{-4}, 1.00×10^{-3}, and 1.00×10^{-2} M. C_{NaCl} was the same, both in CS and PMAA solutions.

2.4. Viscometry. Viscometry of CS/PMAA particulate systems, obtained as described in Section 2.3, was carried out using an Ubbelohde viscometer size 0B, previously calibrated with different fluids. The flow time in these measurements was never shorter than 100 s (the time of bidistilled water being 207.9 ± 0.1s). All of these experiments were conducted at a temperature $T = 25.00 \pm 0.05$ °C.

2.5. Turbidity Measurements. Turbidity measurements of CS/PMAA particulate systems obtained as described in section 2.3 were

Table 1. Intrinsic Viscosity, [η], and k_1 for PMAA with Different Initiator/MAA Mass Ratio

initiator/MAA mass ratio	[η] (dL·g^{-1})	k_1
1.5%	2.9 ± 0.1	0.286 ± 0.005
0.375%	5.0 ± 0.1	0.254 ± 0.001

carried out using a turbidimeter Hach, model 2100P (USA). The instrument was equipped with a tungsten filament lamp, a 90° detector to monitor scattered light, and a transmitted light detector. The instrument's microprocessor calculated the ratio of the signals from 90° and transmitted light detectors, correcting interferences from color- and/or light-absorbing materials. The turbidity of the CS/PMAA particles, which is related to average particle size and particle concentration,[39] was then determined.

2.6. Determination of pH. A Micronal pH meter, model B474 (Brazil), was used for pH determination of the dispersions, after complexation, at room temperature [25 ± 2 °C].

2.7. Zeta Potential Measurements. Electrophoretic mobilities of the CS/PMAA particles (obtained with saltless solutions) were determined at room temperature with dispersions resultant from the re-dispersion of particles obtained by centrifugation. In these measurements, KCl was added to the continuous phase, so that its concentration was 10^{-4} mol·L^{-1}, to maintain a constant ionic strength. The pH of this dispersion was maintained at 4.50 ± 0.05. The electrophoretic mobility measurements, μ_E, were carried out using a Zeta-Meter System 3.0+ (Zeta-Meter Inc., USA). Zeta potential, ζ, of the particles from a given CS/PMAA suspension was calculated from μ_E by employing the Smoluchowski relationship[8]

$$\zeta = \frac{\mu_E \eta}{\epsilon_0 \epsilon_r}$$

where ϵ_0 is the permittivity of a vacuum, ϵ_r is the relative dielectric permittivity of the medium (dielectric constant), and η is the viscosity of the dispersing phase.

2.8. FTIR Characterization of CS/PMAA Particles. FTIR spectra were carried out using a Thermo Nicolet Nexus 470 spectrometer with disks made of CS/PMAA particles pressed with KBr (these particles were separated from the original dispersion via centrifugation, washed with ethanol and dried at room temperature, under vacuum in a desiccator). The operational parameters were as follows: number of scans, 32; resolution, 4 cm^{-1}.

3. Results and Discussion

3.1. MAA Polymerization. The values of intrinsic viscosity, [η], and Huggins constant, k_1, for PMAA obtained with initiator/MAA mass ratio of 1.5 and 0.375% are shown in Table 1. As the amount of initiator decreases, the number of active polymerization centers decreases, increasing, as a consequence, the molecular weight of the polymer,[40] resulting in a higher value of [η]. The values of k_1 for the two systems were in the same range, indicating that, although with different molecular weights, the synthesized polymers had the same hydrodynamic nature (in other words, tridimensionally the same coil geometry).[41] From now on, the polymer with the highest intrinsic viscosity will be referred to as HPMAA and the polymer with lowest intrinsic viscosity as LPMAA.

3.2. FTIR Spectroscopy. FTIR spectra of PMAA, CS/PMAA particles, and CS are shown in Figure 2. The FTIR spectrum of CS itself showed some features of amide groups: amide I and amide II bands at 1647 and 1598 cm^{-1}, respectively. The intense band at 3420 cm^{-1} should be assigned to the stretching vibration of O−H and/or N−H, as well as to intermolecular hydrogen bonding within the polysaccharide.[42] The absorption bands at

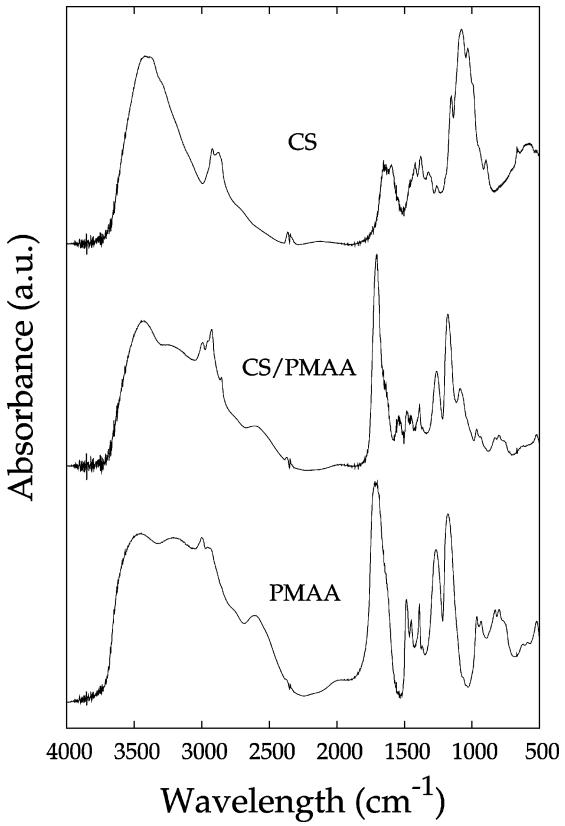

Figure 2. FTIR spectra of chitosan, CS, poly(methacrylic acid), PMAA, and CS/PMAA particles. The $r_{CS/PMAA}$ used was 0.2, and the polyacid was LPMAA.

1154 cm^{-1} (anti-symmetric stretching of the C−O−C bridge), 1078, and 1031 cm^{-1} (skeletal vibrations involving C−O stretching) are characteristic of chitosan's saccharide structure.[43] In the spectrum of PMAA, formation of intramolecular hydrogen bonding may be characterized by a wider band at 3453 cm^{-1}. The presence of bands in the range of 1715−1175 cm^{-1} has been assigned to C−O and C−H stretching vibrations,[42] and the absorption band at 1716 cm^{-1} has been assigned to C═O stretching vibration from carboxylic groups. One can see a shift from 1716 to 1701 cm^{-1} in the spectrum of the CS/PMAA particles, attributed to the carboxyl absorption band from PMAA; the amide bands in the CS spectrum disappear, and a new distinct band appears at 1648 cm^{-1}, which can be assigned to the absorption band of NH^{3+} from CS. Furthermore, the absorption bands at 1542 and 1389 cm^{-1}, present in the spectrum of CS/PMAA particles, resulted from asymmetrical and symmetrical [O−C═O]$^-$ stretching vibrations.[44,45] These results are indicative of complexation between the dissociated carboxylic groups of PMAA and the protonated amino groups of CS by electrostatic interactions, resulting in the polyelectrolyte complex. The spectra did not present different features as a function of PMAA molecular weight.

3.3. Viscometry and Turbidimetry.

3.3.1. Molecular Weight Effect. Figure 3 shows the results obtained from viscosity and turbidity measurements as a function of $r_{CS/PMAA}$ and $r_{NH_2/COOH}$, using the lowest molecular weight PMAA (LPMAA), without the addition of NaCl. As $r_{CS/PMAA}$ is increased, the viscosity increases and reaches a maximum value at $r_{CS/PMAA} = 0.17$. As has already been pointed out in previous works, viscosity data is mainly bound to phenomena which occur in the continuous phase, whereas turbidity data is bound to the formation of solid particles.[46,47] In other words, this increase in viscosity is a result of the formation of soluble

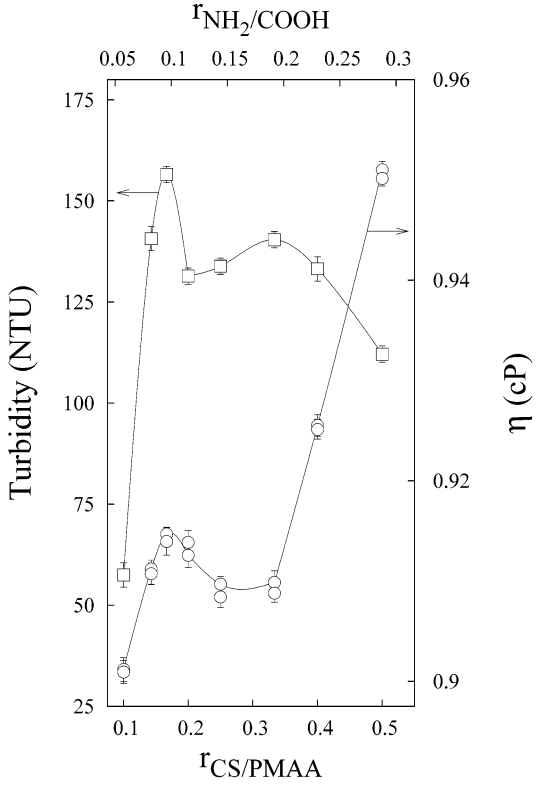

Figure 3. Turbidity (squares), and viscosity, η (circles), of CS/PMAA dispersions as a function of $r_{CS/PMAA}$ and $r_{NH_2/COOH}$ using LPMAA.

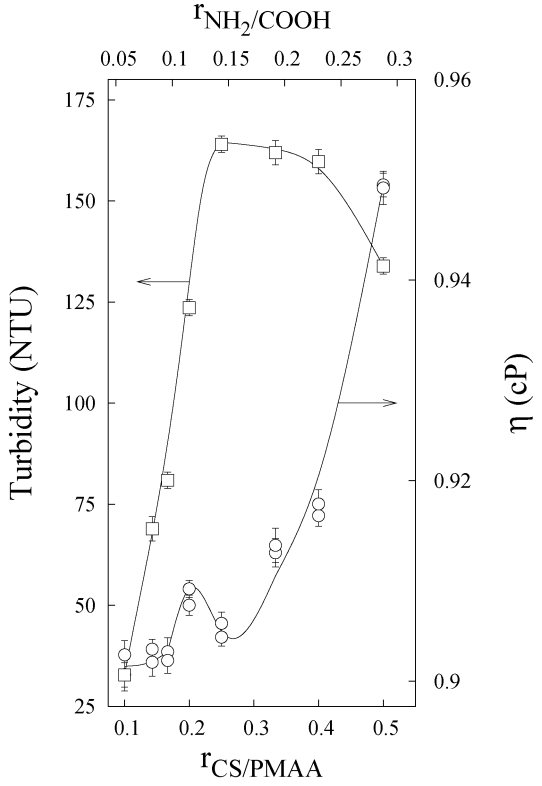

Figure 4. Turbidity (squares), and viscosity, η (circles), of CS/PMAA dispersions as a function of $r_{CS/PMAA}$ and $r_{NH_2/COOH}$ using HPMAA.

complexes, generating macromolecular species with bigger dimensions. The decrease in viscosity (after the maximum) is due to (1) the decrease in the occurrence of complexation and/or (2) the number of polyelectrolyte molecules in the continuous phase. The maximum in turbidity at the same value ($r_{CS/PMAA} = 0.17$) strenghtens these hypotheses, since a maximum in turbidity means a maximum in the occurrence of insoluble complex particles, which come from the continuous phase, resulting in a drastic reduction of macromolecular hydrodynamic volume. Obviously, an increase in turbidity also due to the occurrence of bridging flocculation cannot be unconsidered.[48] Further increase in $r_{CS/PMAA}$ results in a continuous decrease in viscosity, up to $r_{CS/PMAA} = 0.25 \sim 0.33$, which is an indication that the formation of insoluble complex particles is still important. The values of turbidity confirm this hypothesis, since a second maximum is also reached at $r_{CS/PMAA} = 0.33$. For higher values of $r_{CS/PMAA}$, the turbidity continuously decreases (indicating the solubilization of complex particles) and the viscosity continuously increases (indicating a higher number of soluble complex structures). This sort of development of turbidity/viscosity in the formation of these complexes has already been observed.[49,50]

One can find a similar behavior to that described in the last paragraph by examining Figure 4, which depicts the relationship between the CS:PMAA mass ratio, $r_{CS/PMAA}$ (or the NH_2:COOH ratio, $r_{NH_2/COOH}$), viscosity of dispersion, η, and dispersion turbidity, for dispersions prepared using the highest molecular weight PMAA (HPMAA). However, some differences must be realized: the maximum in viscosity now occurs at $r_{CS/PMAA} = 0.2$, with a maximum in turbidity around $r_{CS/PMAA} = 0.25$, although without the same definition found for LPMAA. These results indicate that the complexes formed with HPMAA are more water-soluble, implying complexes formed by LPMAA as having more compacted structures. The higher solubility of HPMAA-based particles may be explained by the fact that LPMAA would have a higher amount of available ionized carboxyl groups per gram. More exactly, a decrease in PMAA molecular weight would imply a higher number of macromolecular coils, which would imply a higher concentration of carboxyl groups at the outer parts of the coils. These carboxyl groups would be more easily ionizable and chitosan would more effectively form macromolecular complexes with these more ionized polyacid molecules. Although HPMAA forms more soluble complexes, another glance at turbidity measurements in Figures 3 and 4 shows that turbidity maximum is more intense in the case of HPMAA. It evidences the formation of larger macromolecular structures with increasing molecular weight of the excess polyanion, as already pointed out by Dautzenberg.[26]

This analysis can be enriched using Figure 5, which depicts the relationship between pH and $r_{CS/PMAA}$ (or $r_{NH_2/COOH}$) for dispersions made with LPMAA and HPMAA. It can be readily noticed that pH for LPMAA is lower than for HPMAA, which is consistent with the assumptions developed in the last paragraph (a higher amount of ionizable carboxyls in LPMAA). The pH of pure PMAA solutions were 3.70 (HPMAA) and 2.95 (LPMAA), whereas the pH of chitosan solutions was 2.60. The values of pH have abruptly decreased from $r_{CS/PMAA} = 0$ to $r_{CS/PMAA} = 0.17 \sim 0.25$ (which characterizes the occurrence of weak acid−base equivalence point): the last range is in coincidence with the maximum in turbidity found for these complexes. As a consequence, the full development of turbidity seems to be bound to an acid−base reaction. At pH $\approx$ 3, the degree of ionization of chitosan is around 1.0,[51] whereas at pH $\approx$ 4, the degree of ionization of PMAA is around 0.2[52] (values obtained for a range of concentrations from 0.01 to 5 wt %). In other words, at these conditions, most of the amino groups of chitosan were in the protonated form, whereas the carboxylic groups of PMAA were in the undissociated form, in equilibrium

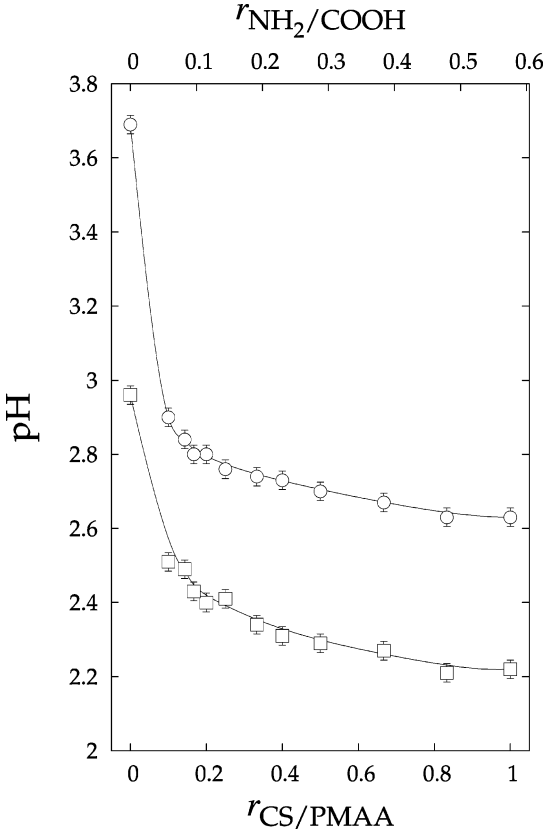

Figure 5. pH as a function of $r_{CS/PMAA}$ and $r_{NH_2/COOH}$ for LPMAA (squares) and HPMAA (circles).

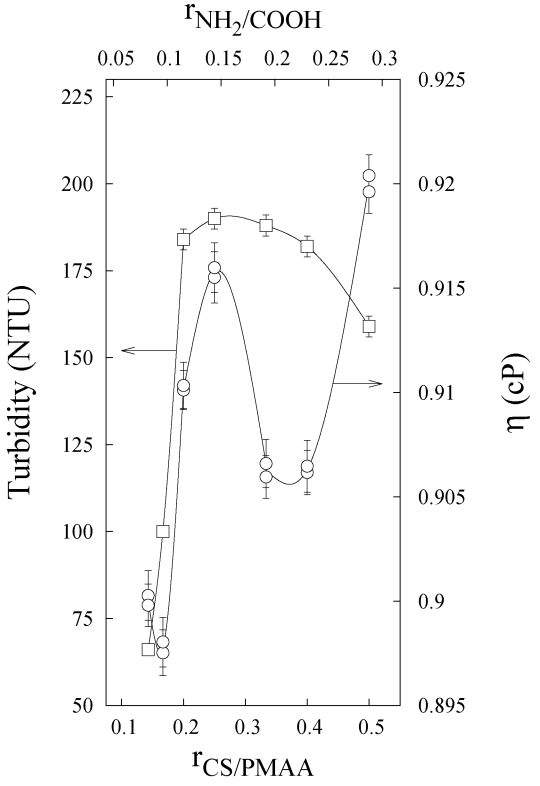

Figure 6. Turbidity (squares), and viscosity, η (circles), of CS/PMAA dispersions as a function of $r_{CS/PMAA}$ and $r_{NH_2/COOH}$ using HPMAA with $C_{NaCl} = 1.00 \times 10^{-4}$ M.

with its dissociated form. Therefore, one can suggest the following complexation reactions:

$$\text{acid ionization: } \sim COOH + H_2O \rightleftharpoons \sim COO^- + H_3O^+$$

$$\text{ionic crosslink formation: } \sim COO^- + {}^+H_3N\sim \rightleftharpoons \sim COO^{-+} H_3N\sim$$

Thus, an increase in PMAA molecular weight (resulting in a lower amount of ionized carboxyl groups at the outer parts of the macromolecular coils) lead to conformational changes at the chain, and consequently, a higher amount of ionic crosslinks of chitosan chains is required for the formation of CS/PMAA polyelectrolyte complexes. This is the reason for the higher values of $r_{CS/PMAA}$ required for reaching a maximum in turbidity for HPMAA. The occurrence of an apparent equivalence point at $r_{CS/PMAA} = 0.2\sim0.25$ ($r_{NH_2/COOH} \approx 0.1$) implies the particles as having a core−shell morphology, the core being rich in CS and the shell rich in PMAA. If $r_{NH_2/COOH} < 1$, it means that there is an excess of COOH groups. If the continuous phase is richer in COOH groups, there is a higher probability that the COOH exceeding groups will be in the shell of the particles. This hypothesis has already been considered in the literature, regarding the formation of different polyelectrolyte complexes.[53,54] As a consequence, there is also the probability of formation of particles by bridging flocculation[6,48] of the negatively charged particles and soluble complex species.

3.3.2. Ionic Strength Effect. Figures 6−8 show the results obtained from viscosity, η, and turbidity, measurements as a function of CS to PMAA mass ratio, $r_{CS/PMAA}$ (or NH_2 to COOH ratio, $r_{NH_2/COOH}$), for different concentrations of NaCl, $C_{NaCl} = 1.00 \times 10^{-4}$, 1.00×10^{-3}, and 1.00×10^{-2} M, respectively. Before analyzing these figures, it is interesting to list the possible effects of increasing low molecular weight electrolyte concentration, C_{NaCl}, on turbidity and viscosity. According to the literature, there are three main effects that may play important roles in the formation of complexes.[48,53,55−57]

1. Increase of C_{NaCl} may screen electrostatic interactions between charges. Thus, the decrease in electrostatic interactions between opposite charges would result in a decrease in the formation of complexed pairs. Turbidity would decrease, the concentration of solubilized macromolecules would increase, and viscosity, depending on the intensity of the polyelectrolyte effect, would increase or decrease.

2. Still regarding the polyelectrolyte effect, the decrease in the repulsion between charges of the same signal (within chitosan and PMAA polyelectrolyte chains) would result in a decrease in dimensions of the solubilized macromolecules. Smaller dimensions, on the other hand, may favor the formation of complex species due to an increase in charge density, as pointed out in section 3.3.1. Turbidity would increase and viscosity would decrease.

3. The increase of C_{NaCl} would result in the precipitation of solubilized complexes, via salting-out effect. As a result, the turbidity would increase and the viscosity would decrease.

Comparing the turbidity behavior observed in Figures 4 ($C_{NaCl} = 0$) and 6 ($C_{NaCl} = 1.00 \times 10^{-4}$ M), one can see that for $C_{NaCl} = 1.00 \times 10^{-4}$ M there is a slight increase in the values turbidity, indicating the prominence of effects (2) and/or (3). The same effects seem to be the most important when C_{NaCl} is increased to 1.00×10^{-3} *M*. However, when C_{NaCl} is increased to 1.00×10^{-2} M, the dispersions become less turbid for all $r_{CS/PMAA}$, indicating the importance of effect (1). If salting out does not play an important role at the highest NaCl concentration, it can be deduced that salting out has no importance in the process of complexation at all.

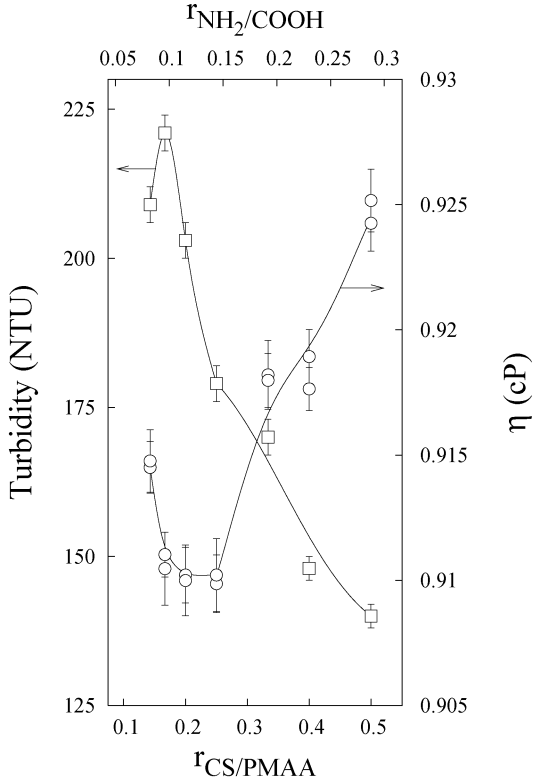

Figure 7. Turbidity (squares), and viscosity, η (circles), of CS/PMAA dispersions as a function of $r_{CS/PMAA}$ and $r_{NH_2/COOH}$ using HPMAA with $C_{NaCl} = 1 \times 10^{-3}$ M.

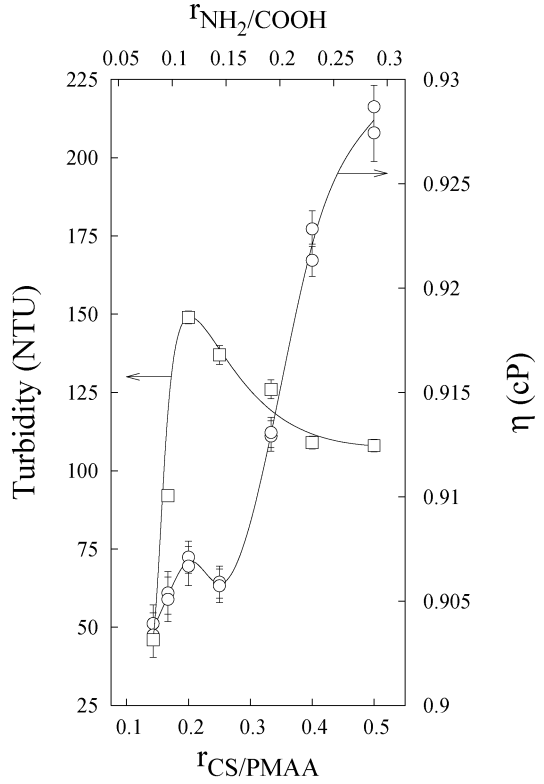

Figure 8. Turbidity (squares), and viscosity, η (circles), of CS/PMAA dispersions as a function of $r_{CS/PMAA}$ and $r_{NH_2/COH}$ using HPMAA with $C_{NaCl} = 1 \times 10^{-2}$ M.

Addition of NaCl decreased the viscosity of the dispersions for all concentrations, which makes effects (1) and (2) possible for all of the systems [since effect (3) has been ruled out]. Additionally, one can see that in Figure 6 there is a minimum in viscosity before it reaches a maximum at $r_{CS/PMAA} \approx 0.25$ (although the shape of the turbidity curve remains the same). This decrease may be related to the occurrence of polyelectrolyte effect [without the formation of complex species, inhibited by the presence of NaCl, effect (1)]. As $r_{CS/PMAA}$ is increased, the formation of complex species results in an increase in viscosity as described earlier in section 3.3.1. Figure 7 shows that an increase in C_{NaCl} to 1.00×10^{-3} M results in the occurrence of a minimum without the presence of a maximum, certainly because the production of a nonsolubilized complex reaches a more defined maximum at $r_{CS/PMAA} = 0.2$ (below $r_{CS/PMAA} \approx 0.25$, indicating that the maximum in viscosity might be shifted to values of $r_{CS/PMAA}$, below the range used in this work). An increase in C_{NaCl} to 1.00×10^{-2} M results in a situation similar to the dispersions without NaCl (although with a lower viscosity, due to the screening effects of the low molecular weight electrolyte). As pointed out in the last paragraph, the viscosity behavior also shows that salting out is not important in this case: for the highest NaCl concentration, solid complex particle formation is disfavored.

3.4. Zeta Potential Measurements. The considerations carried out in the last section can be enriched by the analysis of Figure 9, which shows the values of zeta potential for the CS/PMAA particles obtained from different molecular weight PMAA and chitosan, in saltless solutions. One can see that for both CS/PMAA dispersions surface charge is negative, the CS/PMAA surface charge being less negative for LPMAA complexes. This is consistent with the occurrence of particles with PMAA-rich shells.

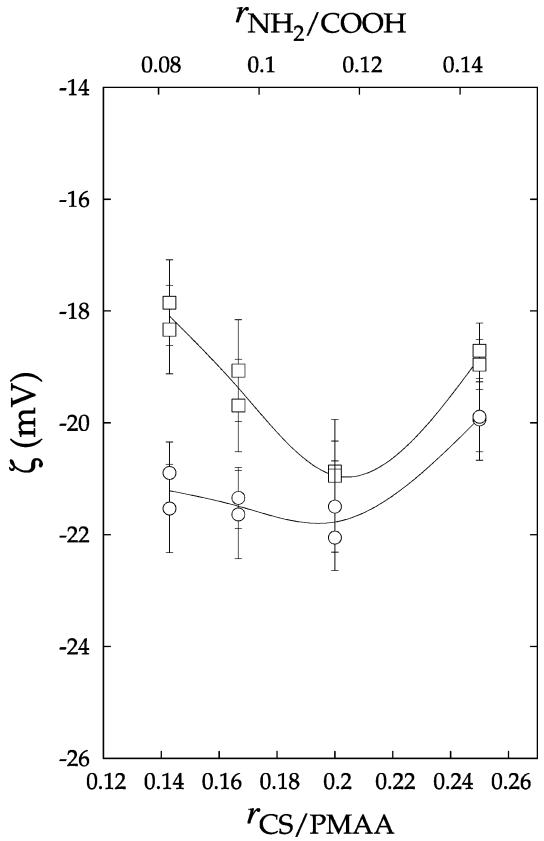

Figure 9. Zeta potential, ζ, as a function of $r_{CS/PMAA}$ and $r_{NH_2/COOH}$ for LPMAA (squares) and HPMAA (circles).

At pH = 2~3, the conditions in which the particles were prepared, one can find complexed chitosan solubilized in the continuous phase and associated to a considerable amount of

undissociated PMAA (which is more important in the case of HPMAA). At pH = 4.5, the conditions used for zeta potential measurements, there is neither PMAA nor solubilized complex species in the continuous phase. The soluble complexes adsorbed on the particles surface would be resolubilized in the continuous phase and initially undissociated carbonyl groups on the surface would then dissociate (as a result of both lower concentration of PMAA in the continuous phase and higher pH). As a consequence, as observed in our experiments, the zeta potential would be lower for HPMAA-based particles (the ones with a higher amount of undissociated carboxyls on the surface). The acid pH, resultant from the re-dispersion of the particles in water, corroborates this hypothesis.

One can also observe that, for both classes of particles, initially the zeta potential decreases with increasing $r_{CS/PMAA}$, indicating an increase in the amount of solubilized macromolecular complex species on the particle surface (and, as a consequence, of initially undissociated carboxyls). For LPMAA, the zeta potential reaches a minimum at $r_{CS/PMAA} = 0.2$, indicating that most of the carboxyls from the shell must be undissociated at this value of $r_{CS/PMAA}$ (at pH = 2∼3, the conditions in which the particles were initially obtained), whereas for HPMAA particles, the zeta potential does not change so abruptly within the range of $0.14 \leq r_{CS/PMAA} \leq 0.2$, certainly due to a much higher number of undissociated carboxyl groups after complexation (at pH = 2∼3) and then increases in the same way observed for the LPMAA-related particles. The increase in zeta potential is correlated to an increase in the formation of complex pairs (which means a decrease in the amount of undissociated carbonyls). It is worthwhile noticing that, around this value of $r_{CS/PMAA}$, the maximum in turbidity was detected for LPMAA-based complexes.

4. Conclusion

CS/PMAA aqueous dispersions had some of their properties influenced by the molecular weight of PMAA and ionic strength. The increase in PMAA molecular weight seemed to increase the solubility of the macromolecular complexes. This increase in solubility must be the result of a lower presence of carboxyl groups at the outer parts of the PMAA macromolecular coils (more easily ionized than the inner ones) as a result of the increase of molecular weight. The occurrence of a more negatively charged particle surface may also increase the formation of complex particles via solubilized complex-driven bridging flocculation. The increase in ionic strength had two effects in the formation of insoluble complexes: at lower concentrations, it favored the formation of these complexes through the decrease in the dimensions of the polyelectrolyte molecules (increase in surface charge density); at higher concentrations, it inhibited the formation of these complexes, possibly due to screening of electrostatic attraction between COO^- and NH_3^+ moieties.

Acknowledgment. The authors thank Brazil's Conselho Nacional de Desenvolvimento Científico e Tecnológico (CNPq), Ministério da Ciência e Tecnologia (MCT), Fundação Coordenação de Aperfeiçoamento de Pessoal de Nível Superior (CAPES), and Pró-Reitoria de Pesquisa da Universidade Federal do Rio Grande do Norte (PROPESQ-UFRN) for financial support during the course of this work.

References and Notes

(1) Dickinson, E. *Food Hydrocolloids* **2003**, *17*, 25−39.
(2) Shahidi, N.; Teymour, F.; Arastoopour, H. *Polymer* **2004**, *45*, 5183−5190.
(3) Tarvainen, M.; Peltonen, S.; Mikkonen, H.; Elovaara, M.; Tuunainen, M.; Paronen, P.; Ketolainen, J.; Sutinen, R. *J. Controlled Release* **2004**, *96*, 179−191.
(4) Wagberg, L.; Nygren, I. *Colloid Surf. A* **1999**, *159*, 3−15.
(5) Coombes, A. G. A.; Breeze, V.; Lin, W.; Gray, T.; Parker, K. G.; Parker, T. *Biomaterials* **2001**, *22*, 1−8.
(6) de Vasconcelos, C. L.; de Medeiros, D. W. O.; de Moura, K. T.; Acchar, W.; Dantas, T. N. C.; Pereira, M. R.; Fonseca, J. L. C. *Powder Technol.* **2003**, *133*, 164−170.
(7) de Vasconcelos, C. L.; de Moura, K. T.; Morais, W. A.; Dantas, T. N. C.; Pereira, M. R.; Fonseca, J. L. C. *Colloid Polym. Sci.* **2005**, *283*, 413−420.
(8) de Vasconcelos, C. L.; Dantas, T. N. C.; Pereira, M. R.; Fonseca, J. L. C. *Colloid Polym. Sci.* **2004**, *282*, 596−601.
(9) Peula-García, J. M.; Molina-Bolivar, J. A.; Velasco, J.; Rojas, A.; Galisteo-González, F. *J. Colloid Interface Sci.* **2002**, *245*, 230−236.
(10) Qiu, X.; Leporatti, S.; Donath, E.; Möhwald, H. *Langmuir* **2001**, *17*, 5375−5380.
(11) Shimono, N.; Takatori, T.; Ueda, M.; Mori, M.; Higashi, Y.; Nakamura, Y. *Int. J. Pharm.* **2002**, *245*, 45−54.
(12) van der Lubben, I. M.; Verhoef, J. C.; Borchard, G.; Junginger, H. E. *Adv. Drug Delivery Rev.* **2001**, *52*, 139−144.
(13) Hans, M. L.; Lowman, A. M. *Curr. Opin. Solid State Mater. Sci.* **2002**, *6*, 319−327.
(14) Dumitriu, S.; Chornet, E. *Adv. Drug Delivery Rev.* **1998**, *31*, 223−246.
(15) Agnihotri, S. A.; Mallikarjuna, N. N.; Aminabhavi, T. M. *J. Controlled Release* **2004**, *100*, 5−28.
(16) Kurita, K. *Polym. Degrad. Stab.* **1998**, *59*, 117−120.
(17) Muroga, Y.; Yoshida, T.; Kawaguchi, S. *Biophys. Chem.* **1999**, *81*, 45−57.
(18) Thanou, M.; Verhoef, J. C.; Junginger, H. E. *Adv. Drug Delivery Rev.* **2001**, *52*, 117−126.
(19) Luessen, H. L.; de Leeuw, B. J.; Pérard, D.; Lehr, C.-M.; de Boer, A. G.; Verhoef, J. C.; Junginger, H. E. *Eur. J. Pharm. Sci.* **1996**, *4*, 117−128.
(20) Borchard, G.; Luessen, H. L.; de Boer, A. G.; Verhoef, J. C.; Lehr, C. M.; Junginger, H. E. *J. Controlled Release* **1996**, *39*, 131−138.
(21) Noach, A. B. J.; Kurosaki, Y.; Blom-Roosemalen, M. C. M.; de Boer, A. G.; Breimer, D. D. *Int. J. Pharm.* **1993**, *90*, 229−237.
(22) Becherán-Marón, L.; Peniche, C.; Argüelles-Monal, W. *Int. J. Biol. Macromol.* **2004**, *34*, 127−133.
(23) Janes, K. A.; Alonso, M. J. *J. Appl. Polym. Sci.* **2003**, *88*, 2769−2776.
(24) Ko, J. A.; Park, H. J.; Hwang, S. J.; Park, J. B.; Leen, J. S. *Int. J. Pharm.* **2002**, *249*, 165−174.
(25) Bouyer, F.; Robben, A.; Yu, W. L.; Borkovec, M. *Langmuir* **2001**, *17*, 5225−5231.
(26) Dautzenberg, H. *Macromolecules* **1997**, *30*, 7810−7815.
(27) Starodubtsev, S. G.; Dembo, A. T.; Dembo, K. A. *Langmuir* **2004**, *20*, 6599−6604.
(28) Dragan, S.; Cristea, M. *Polymer* **2002**, *43*, 55−62.
(29) Wang, H.; Li, W.; Lu, Y.; Wang, Z. *J. Appl. Polym. Sci.* **1997**, *65*, 1445−1450.
(30) Nge, T. T.; Yamaguchi, M.; Hori, N.; Takemura, A.; Ono, H. *J. Appl. Polym. Sci.* **2002**, *83*, 1025−1035.
(31) Wang, H.; Li, W.; Lu, Y.; Wang, Z.; Zhong, W. *J. Appl. Polym. Sci.* **1996**, *61*, 2221−2224.
(32) Prashanth, K. V. H.; Kittur, F. S.; Tharanathan, R. N. *Carbohydr. Polym.* **2002**, *50*, 27−33.
(33) Smith, G. B.; Russell, G. T.; Yin, M.; Heuts, J. P. A. *Eur. Polym. J.* **2005**, *41*, 225−230.
(34) Fernandes, A. L. P.; Martins, R. R.; da Trindade Neto, C. G.; Pereira, M. R.; Fonseca, J. L. C. *J. Appl. Polym. Sci.* **2003**, *89*, 191−196.
(35) Taylor, T. J.; Stivala, S. S. *Polymer* **1996**, *37*, 715−719.
(36) Hu, H.; He, T.; Feng, J.; Chen, M.; Cheng, R. *Polymer* **2002**, *43*, 6357−6361.
(37) de Vasconcelos, C. L.; Pereira, M. R.; Fonseca, J. L. C. *J. Appl. Polym. Sci.* **2001**, *80*, 1285−1290.
(38) Melis, S.; Kemmerer, M.; Meuldijk, J.; Storti, G.; Morbidelli, M. *Chem. Eng. Sci.* **2000**, *55*, 3101−3111.
(39) Peaker, F. W. *Analyst* **1960**, *85*, 235−244.
(40) Lyoo, W. S.; Do Ghim, H.; Yoon, W. S.; Lee, J.; Lee, H. S.; Ji, B. C. *Eur. Polym. J.* **1999**, *35*, 647−653.

(41) Harding, S. E.; Day, K.; Dhami, R.; Lowe, P. M. *Carbohydr. Polym.* **1997**, *32*, 81−87.
(42) Sun, T.; Xu, P. X.; Liu, Q.; Xue, J. A.; Xie, W. *Eur. Polym. J.* **2003**, *39*, 189−192.
(43) Peniche, C.; Elvira, C.; Roman, J. S. *Polymer* **1998**, *39*, 6549−6554.
(44) Peniche, C.; Arguelles-Monal, W.; Davidenko, N.; Sastre, R.; Gallardo, A.; San Román, J. *Biomaterials* **1999**, *20*, 1869−1878.
(45) Hu, Y.; Jiang, X.; Ding, Y.; Ge, H. X.; Yuan, Y.; Yang, C. *Biomaterials* **2002**, *23*, 3193−3201.
(46) da Trindade Neto, C. G.; Fernandes, A. L. P.; Santos, A. I. B.; Morais, W. A.; Navarro, M. V. M.; Dantas, T. N. C.; Pereira, M. R.; Fonseca, J. L. C. *Polym. Int.* **2005**, *54*, 659−666.
(47) Fernandes, A. L. P.; Morais, W. A.; Santos, A. I. B.; de Araujo, A. M. L.; dos Santos, D. E. S.; dos Santos, D. S.; Pavinatto, F. J.; Oliveira, O. N.; Dantas, T. N. C.; Pereira, M. R.; Fonseca, J. L. C. *Colloid Polym. Sci.* **2005**, *284*, 1−9.
(48) de Vasconcelos, C. L.; Pereira, M. R.; Fonseca, J. L. C. *J. Dispersion Sci. Technol.* **2005**, *26*, 59−70.
(49) Gamzazade, A. I.; Nasibov, S. M. *Carbohydr. Polym.* **2002**, *50*, 339−343.
(50) Mende, M.; Petzold, G.; Buchhammer, H. M. *Colloid Polym. Sci.* **2002**, *280*, 342−351.
(51) Chavasit, V.; Kienzle-Sterzer, C.; Torres, J. A. *Polym. Bull.* **1988**, *19*, 223−230.
(52) Shih, C. J.; Hon, M. H. *J. Eur. Ceram. Soc.* **1999**, *19*, 2773−2780.
(53) Schatz, C.; Lucas, J. M.; Viton, C.; Domard, A.; Pichot, C.; Delair, T. *Langmuir* **2004**, *20*, 7766−7778.
(54) Dragan, E. S.; Schwarz, S. *J. Polym. Sci., Polym. Chem. Ed.* **2004**, *42*, 2495−2505.
(55) Dautzenberg, H.; Jaeger, W. *Macromol. Chem. Phys.* **2002**, *203*, 2095−2102.
(56) Dedinaite, A.; Ernstsson, M. *J. Phys. Chem. B* **2003**, *107*, 8181−8188.
(57) Dragan, S.; Cristea, M. *Eur. Polym. J.* **2001**, *37*, 1571−1575.

BM050963W